Water Research 265 (2024) 122275

Contents lists available at ScienceDirect

Water Research

journal homepage: www.elsevier.com/locate/watres

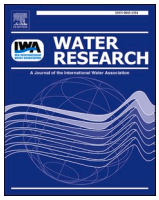

Emergency control of dinoflagellate bloom in freshwater with chlorine enhanced by solar radiation: Efficiency and mechanism

Ru Wang [a,b], Ya Cheng [a,b], Qiqi Wan [a,b], Ruihua Cao [a,b], Jie Cai [a,b], Tinglin Huang [a,b,c], Gang Wen [a,b,c,*]

[a] Shaanxi Provincial Field Scientific Observation and Research Station of Water Quality in Qinling Mountains, Xi'an University of Architecture and Technology, Xi'an 710055, PR China
[b] Shaanxi Key Laboratory of Environmental Engineering, Xi'an University of Architecture and Technology, Xi'an 710055, PR China
[c] Collaborative Innovation Center of Water Pollution Control and Water Quality Security Assurance of Shaanxi Province, Xi'an University of Architecture and Technology, Xi'an 710055, PR China

ARTICLE INFO

Keywords:
Peridinium umbonatum
Solar/chlorine
Enhanced
Influencing factors
Apoptosis mechanism

ABSTRACT

Dinoflagellate requires a lower temperature and blooms frequently in the spring and autumn compared to regular cyanobacteria. The outbreak of dinoflagellate bloom will also lead to the death of some aquatic organisms. However, research on freshwater dinoflagellates is still lacking due to the challenges posed by classification and culture in laboratory. The removal effect and mechanism of *Peridinium umbonatum* (*P. umbonatum*, a typical dinoflagellate) were investigated using solar/chlorine in this study. The effect of simulated solar alone on the removal of algae was negligible, and chlorine alone had only a slight effect in removing algae. However, solar/chlorine showed a better removal efficiency with shoulder length reduction factor and k_{max} *enhancement factor* of 2.80 and 3.8, respectively, indicating a shorter latency period and faster inactivation rate for solar/chlorine compared to solar and chlorine alone. The removal efficiency of algae gradually increased with the chlorine dosage, but it dropped as the cell density grew. When the experimental temperature was raised to 30 °C, algal removal efficiency significantly increased, as the temperature was unsuitable for the survival of *P. umbonatum*. Attacks on cell membranes by chlorine and hydroxyl radicals (•OH) produced by solar/chlorine led to a decrease in cell membrane integrity, leading to a rise in intracellular reactive oxygen species and an inhibition of photosynthetic and antioxidant systems. Cell regeneration was not observed in either the chlorine or solar/chlorine systems due to severe cell damage or cysts formation. In addition, natural solar radiation was demonstrated to have the same enhancing effect as simulated solar radiation. However, the algal removal efficiency of solar/chlorine in real water was reduced compared to 119 medium, mainly due to background material in the real water substrate that consumed the oxidant or acted as shading agents.

1. Introduction

Harmful algal blooms occur worldwide and pose potential risks to human health and ecosystems. Cyanobacterial and chlorophyta are the most frequently studied freshwater algae because they are more prevalent (Li et al., 2020; Wang et al., 2024; Yu et al., 2024; Zhang et al., 2022). In fact, freshwater dinoflagellate blooms have been discovered to be widespread in lakes and reservoirs with cell densities of 10^5~10^7 cells/L, and they can cause a variety of ecological security and water supply issues (Table S1). The blooms extend over time and location scales, negatively affecting the lives of coastal residents and the production of enterprises, including odors, toxins, and water supply security (Ginzburg et al., 1998; Oshima et al., 1987; Roset et al., 2002). Therefore, freshwater dinoflagellate blooms and their control should not be overlooked.

The nucleus of the dinoflagellate has a unique structure in the absence of histones and nucleosomes, and the terms mesokaryotic and dinokaryotic have been used for this unique nucleus. The algal cells are generally spherical, ovate and polygonal, with a cellulose plate-like wall and two flagella (Carty and Parrow, 2015). Emergency control, which includes physical, chemical and biological techniques, is mostly applied for sudden algal bloom events. Mature control methods have been

* Corresponding author.
E-mail address: hitwengang@163.com (G. Wen).

https://doi.org/10.1016/j.watres.2024.122275
Received 30 May 2024; Received in revised form 5 August 2024; Accepted 13 August 2024
Available online 14 August 2024

developed due to the regular occurrence of cyanobacterial blooms. However, control techniques for dinoflagellates cannot be fully adapted from those used for cyanobacterial because of their larger shape and more complicated cellular structure. For instance, pressure and ultrasonic are less effective for dinoflagellate because they attack mainly on the gas vacuoles of cyanobacteria, which are absent in dinoflagellate (Li et al., 2022). Currently, ultraviolet (UV) and hydrodynamic controls have been found to be effective in controlling dinoflagellate blooms. All *Peridinium bipes* died after 48 and 6 h of continuous exposure to UV doses greater than 80 and 2400 μW/cm^2, respectively (Kawabata et al., 1990). Based on the findings, Iseri et al. (1994) developed a boat with a UV-C system, successfully eliminating a *P.bipes* bloom in a Japanese reservoir, and the radiation intensity was greater than 2400 μW/cm^2. Song et al. (2021) analyzed the thresholds for flow velocities, Reynolds numbers, and mixing layer depth/euphotic zone for the Zipingpu Reservoir and noted that either accelerating horizontal flow or facilitating vertical mixing can prevent dinoflagellate blooms. The water-lifting aerator has been successfully applied to the spring dinoflagellate bloom control in Lijiahe Reservoir (Huang et al., 2022). The concentration of oxidants required for controlling dinoflagellate is also higher than that for cyanobacteria. Ichikawa et al. (1992) found that all cysts of *Alexandrium tamarense* exposed to 30 mg/L hydrogen peroxide (H_2O_2) for 48 h showed protoplasm contraction and decolorization. After 48 h of treatment with 50.0 mg/L of H_2O_2, the cell density of *Alexandrium ostenfeldii* in actual water bodies decreased by 99.8 % (Burson et al., 2014). *P. umbonatum* did not exhibit a significant decrease in photosynthetic activity following treatment with 8 mg/L $KMnO_4$ for 30 min (pH = 3.0) or 1.5 mg/L O_3 (Gong, 2022). However, previous studies have shown that 3 mg/L sodium percarbonate is effective in controlling filamentous cyanobacteria throughout the water column (Xu et al., 2021), and 10.0 mg/L H_2O_2 is effective in controlling cyanobacterial blooms (Zhou et al., 2020, 2018). Regarding biological methods, it was shown that certain strains had substantial algicidal activities against *dinoflagellate* (Hu et al., 2020; Kang et al., 2008). But there are few successful applications of biological control in practice. In summary, research on freshwater algal control techniques remains insufficient.

In recent years, solar disinfection (SODIS) has gained popularity as a water disinfection technique (Xia et al., 2022). Advanced oxidation processes (AOPs) based on solar energy, such as solar/chlorine and solar/H_2O_2, have attracted a lot of interest in water treatment recently (Rodríguez-Chueca et al., 2019). Photolysis of free chlorine by UV wavelengths in solar produces hydroxyl radical (•OH) and ozone (O_3) with equations as shown in Eqs. (1)-(3) (Forsyth et al., 2013). Previous studies have reported the higher inactivation of bacterial and fungal spores by solar/chlorine due to the simultaneous attack by •OH and O_3 (Forsyth et al., 2013; Wan et al., 2022; Zhou et al., 2014). Moreover, solar-based AOPs have been applied to algae control processes. Ye et al. (2023) reported that the solar/periodate system could inhibit *Microcystis aeruginosa* by reducing photosynthetic activity and reduce the release of intracellular microcystins due to its high selectivity to the cell membrane. In direct sunlight, •OH is generated from H_2O_2 and irreversibly damages *Pseudanabaena* sp. (Wang et al., 2017a). Piel et al. (2019) reported that even low H_2O_2 concentrations can be highly effective if cyanobacteria are exposed to high light intensities and recommended performing lake treatments during sunny days. However, relevant studies have also been focused on cyanobacteria, and there were no reports on the effectiveness of solar/chlorine in controlling freshwater dinoflagellate.

$$HOCl/OCl^- + h\nu \rightarrow HO\bullet/O^{\bullet-} + Cl\bullet \quad (1)$$

$$OCl^- + h\nu \rightarrow O(^3P) + Cl^- \quad (2)$$

$$O(^3P) + O_2 \rightarrow O_3 \quad (3)$$

In this study, the predominant dinoflagellate, *P. umbonatum*, was chosen because it was the dominant algal species during the bloom period in Feitsui Reservoir. (Wu and Chou, 1998). The study aimed to (1) assess the removal efficiency of algae by solar/chlorine and compare it with solar and chlorine alone treatment; (2) evaluate the effect of different factors on the removal efficiency of solar/chlorine; (3) analyze the enhancement mechanisms of solar/chlorine treatment; (4) evaluate the regrowth of *P. umbonatum* after different treatments.

2. Materials and methods

2.1. Chemicals and materials

Sodium hypochlorite (NaOCl) was purchased from Sigma-Aldrich and the H_2O_2 was purchased from Slnopharm Chemical Reagent Co., Ltd. (China). Other reagents were purchased from Kermel Chemical Reagent Co., Ltd. (China). Milli-Q water (Millipore, USA) was used to prepare all of the solutions. The N, N-diethyl-p-phenylenediamine (DPD) technique was used to measure the concentration of chlorine (Wang et al., 2021). The concentration of H_2O_2 in the stock solution was verified using potassium permanganate titration (Zhou et al., 2020).

2.2. Preparation of algal suspension

Peridinium umbonatum (FACHB-329) was cultured in improved 119 media after being purchased from the Institute of Hydrobiology, Chinese Academy of Sciences. The cultures were incubated at 25 °C in an incubator with 12 h light and 12 h dark cycles (2000 lux) (MGC-250P, Bluepard instrument) (Xu et al., 2016). Algal cells were used in experiments after being cultivated for 30–40 days.

2.3. Experimental procedure

Algal suspension with an initial scell density of (1.0 ± 0.2) × 10^4 cells/mL was added to the double-walled beaker and exposed to simulated solar radiation with an intensity of 900 W/m^2 (300–800 nm) (HF-X300DUV, China) (Fig. S1, S2). The solar/chlorine experiment was initiated by adding NaOCl stock solution to the beaker under solar radiation. The experimental temperature was controlled by a low constant temperature water bath (DC0506, Hefan, China). The equipment was turned on and warmed up for 30 min before the experiment. Samples were collected at intervals and immediately quenched using 0.1 M $Na_2S_2O_3$ (Wan et al., 2020). The chlorine dose (2.0, 3.0, 4.0 mg/L) and temperature (20, 25, 30 °C) were adjusted to investigate the dependence of the algal removal effect on the oxidant dose and temperature. Different concentrations of *P.umbonatum* (1.0 × 10^4, 2.0 × 10^4, 3.0 × 10^4 cells/mL) were added to study the effect of initial concentration on the algal control. Samples were collected for activity analysis and counting. All experiments were carried out in triplicate.

2.4. Analytical methods

2.4.1. Cell integrity

The algal cells were enumerated using a hemocyte counting plate and observed using a microscope. SYTOX was utilized to stain algae and assess the integrity of the cell membrane via fluorescence microscopy (BX51, Olympus, Japan) (Daly et al., 2007; Tian et al., 2021). A mixture of 0.3 mL of algal solution and 5.0 μmol/L of SYTOX stain was prepared, and the stained algal solution was incubated in the dark for 20–30 min. The final concentration of SYTOX dye was adjusted to 0.1 μmol/L (Xie et al., 2013). Subsequently, 100 μL algal solution was placed on a counting plate, and the integrity of the algal membrane was detected through blue fluorescence (488 nm) using a fluorescence microscope.

Algal cells were photographed with a scanning electron microscope (SEM) (GeminiSEM500, ZEISS, Germany) to observe morphological changes during the reaction. The detailed treatment followed previous works (Tian et al., 2021; Wen et al., 2020).

2.4.2. Photosynthetic activity

Chlorophyll-a (Chl-a), the maximum optical quantum yield (Fv/Fm), effective quantum yield of photosynthetic system II (Y(II)) and relative electron transport rate (ETR) were examined to assess the state of the photosynthetic system. Chl-a, a significant pigment involved in photosynthetic processes, was extracted by absolute ethyl alcohol and ultrasonic treatment. The concentration was measured at 630, 645, 663, and 750 nm by a spectrophotometer and calculated with Eq. (4) (Holm--Hansen and Riemann, 1978; Pápista et al., 2002). Additionally, 1.5 mL of algal solution was taken in a 1.5 mL centrifuge tube after the certain reaction time. The centrifuge tubes were placed in black centrifuge tube racks for 10–15 min in a dark environment, and then the photosynthetic activity of algal cells was determined by the IMAGING-PAM chlorophyll fluorescence imaging system (WALZ, Germany) (Xu et al., 2016).

$$Chla\ (\mu g/L) = \frac{V_1 \cdot [11.64 \times (D_{663} - D_{750}) - 2.16 \times (D_{645} - D_{750}) + 0.1 \times (D_{630} - D_{750})]}{V \cdot L} \quad (4)$$

Where V_1 is volume of colorimetric tubes (mL), V is volume of sample (L), L is optical path of cuvette (1 cm), D_{630}, D_{645}, D_{663} and D_{750} are the absorbance at 630 nm, 645 nm, 663 nm and 750 nm, respectively.

2.4.3. Antioxidant system

5 mL of algal solution was added to a sterilized centrifuge tube to extract crude enzyme solution (Text S1) and determine the activity of superoxide dismutase (SOD) with a total superoxide dismutase assay kit (WST-1) (Zhang et al., 2022).

2.4.4. Determination of organic matter

Total organic carbon (TOC-L, Shimadzu, Japan) was used to examine the dissolved organic carbon (DOC). The excitation-emission matrix spectra (EEM) of samples were measured using a fluorescence spectrophotometer (F-7000, Hitachi, Japan). The detailed procedures refer to the previous works and are described in Text S2 (Han et al., 2022; Jutaporn et al., 2020). All samples were filtered with a 0.22 μm membrane before the measurement.

2.5. Inactivation kinetics

The effectiveness of algal control was evaluated by the removal efficiency, which was calculated as shown in Eq. (5). The Geeraerd and Van Impe inactivation model-fitting tool (GInaFiT) was used to fit the decay process of *P.umbonatum* (Geeraerd et al., 2005). The 'log-linear with a shoulder' model and the 'log-linear with a shoulder and a tail' model were explained in Eqs. (6)-(7). According to Forsyth et al. (2013), the enhanced effect of solar radiation was assessed based on the SL reduction factor and the *k* enhancement factor (Eqs. (8)-(9)).

$$\text{Removal efficiency} = \frac{N_0 - N}{N_0} \quad (5)$$

$$N = N_0 \cdot e^{(-k_{max}) \cdot t} \cdot \frac{e^{k_{max} \cdot SL}}{1 + (e^{k_{max} \cdot SL} - 1) \cdot e^{(-k_{max}) \cdot t}} \quad (6)$$

$$N = (N_0 - N_{res}) \cdot e^{(-k_{max}) \cdot t} \cdot \frac{e^{k_{max} \cdot SL}}{1 + (e^{k_{max} \cdot SL} - 1) \cdot e^{(-k_{max}) \cdot t}} + N_{res} \quad (7)$$

$$\text{SL reduction factor} = \frac{SL_0}{SL} \quad (8)$$

$$k \text{ enhancement factor} = \frac{k_{max}}{k_{max0}} \quad (9)$$

Where N_0 and N are the initial cell density of *P.umbonatum* ($\times 10^4$ cells/mL) and the cell density ($\times 10^4$ cells/mL) at the time t (h), respectively; N_{res} is the cell density in the trailing phase ($\times 10^4$ cells/mL); k_{max} is the maximum rate constant (h^{-1}) and SL is the shoulder length (h). SL_0 and SL represent the shoulder length in chlorine and solar/chlorine systems (h); k_{max0} and k_{max} represent the maximum inactivation rate constant in chlorine and solar/chlorine systems (h^{-1}).

The quality of fit for the models was evaluated using the root mean sum of squared errors (RMSE) and the coefficient of determination (R^2). A better fit is indicated by values of R^2 closer to 1 and RMSE closer to 0.

3. Results and discussion

3.1. Effectiveness of solar, chlorine and solar/chlorine processes

Fig. 1 compared the control effect of *P. umbonatum* in solar/H_2O_2 and solar/chlorine systems with 900 W/m^2 of solar radiation. The initial concentrations of H_2O_2 and chlorine were 10.0 mg/L and 3.0 mg/L, respectively. As shown in Fig. 1(a) and S3, exposure to H_2O_2 alone and solar radiation alone had negligible effects on *P. umbonatum*. The enhancement of H_2O_2 by solar radiation was limited and the removal efficiency was only 20 % after 8 h. H_2O_2 is commonly used in the control of blue-green algae blooms with favorable results due to its safety and environmental friendliness (Chen et al., 2021; Zhou et al., 2020, 2018). However, the efficiency of H_2O_2 is impoverished in dinoflagellate because of their complicated cellular structure: (1) the morphology of algae cells is larger than that of cyanobacteria; (2) the cell wall is a thicker and platelike structure composed of cellulose, which may consume oxidizing chemicals and protect the cells from damage (Carty and Parrow, 2015).

Chlorine is frequently used in microbial control as a powerful oxidant and produces oxidizing reactive species under solar radiation. Therefore, this study utilized chlorine to achieve emergency control of *P. umbonatum* and explore the enhanced effects of solar. Images depicting algal cell deterioration with solar/chlorine treatment were shown in Fig. S4. The kinetic parameters fitted by GInaFiT for *P. umbonatum* were shown in Table 1. The 'log-linear with a shoulder' and 'log-linear with a shoulder and a tail' models provided a suitable fit for the inactivation of chlorine alone and the solar/chlorine treatment, respectively. The primary explanation for the 'lag phase' (indicated by SL) is that the algae cells exhibit a degree of tolerance to oxidative damage (Cao et al., 2022). The SL and k_{max} in chlorine alone treatment were 10.22 h and 0.29 h^{-1}, respectively. The SL and k_{max} of solar/-chlorine treatment were 3.65 h and 1.11 h^{-1}, respectively. According to Eqs. (3)-(4), the SL reduction factor and k_{max} enhancement factor have been calculated to be 2.80 and 3.8, respectively. The enhancement of chlorine by solar was mainly due to a decrease in the lag phase and an increase in the reaction rate.

3.2. Influencing factors

The effects of chlorine dose on the effectiveness of the solar/chlorine system were summarized in Fig. 2(a) and S5(a). The removal efficiency increased as the chlorine dose was raised from 2.0 mg/L to 4.0 mg/L. After 8 h, the removal efficiency of *P. umbonatum* under 2.0 mg/L solar/chlorine conditions was only 33 %. However, the removal efficiency increased to 75 % and 85 % when the concentration was increased to 3.0 mg/L and 4.0 mg/L, respectively. With the concentration of chlorine increased from 2.0 to 4.0 mg/L, the SL of *P. umbonatum* decreased from

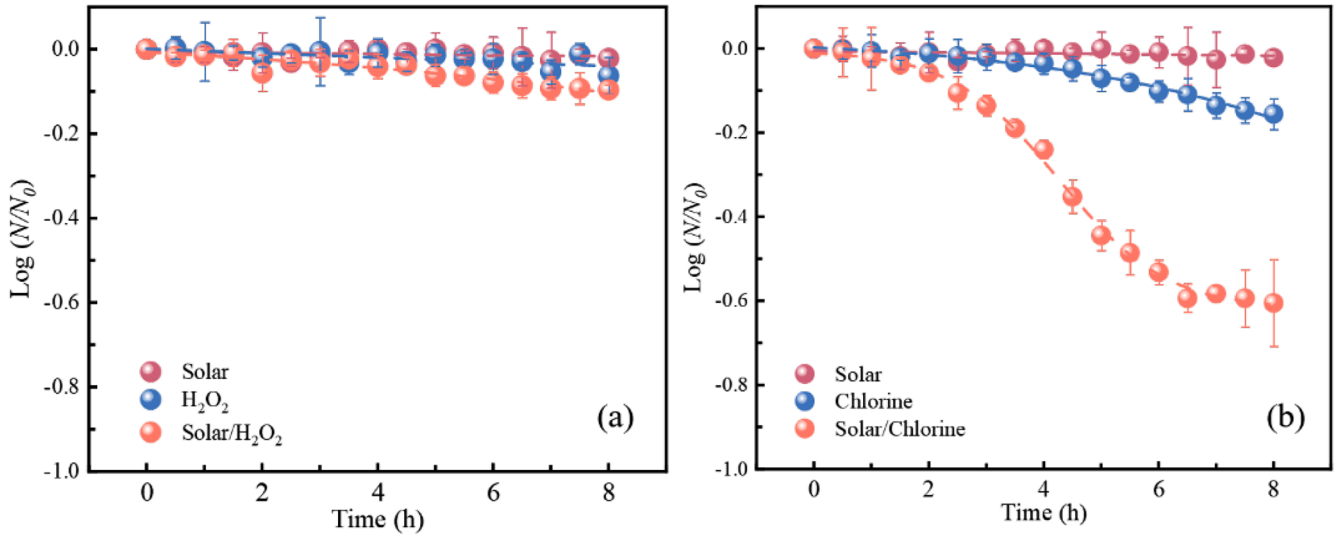

Fig. 1. The kinetic fitting curve of *P. umbonatum* in (a) solar/H_2O_2 and (b) solar/Cl_2 treatments. Conditions: initial *P. umbonatum* concentration = (1.0 ± 0.2)×10^4 cells/mL; $[H_2O_2]_0$ = 10.0 mg/L; $[chlorine]_0$ = 3.0 mg/L; solar irradiance = 900 W/m^2; T = 25±2 °C; pH = 6.8 ± 0.2.

Table 1
Inactivation kinetic parameters of the *P. umbonatum*.

Inactivation methods	SL (h)	k_{max}(h^{-1})	R^2	RMSE	*k* enhancement factor	SL reduction factor
Chlorine	10.22±0.22	0.29±0.03	0.9850	0.0070		
Solar/Chlorine	3.65±0.08	1.11±0.07	0.9972	0.0141	3.8	2.80

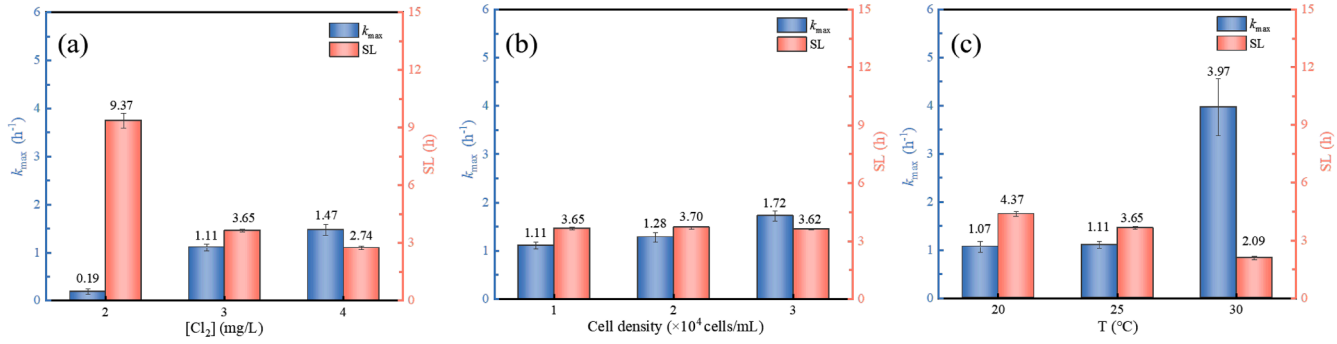

Fig. 2. Effect of (a) chlorine concentration (b) initial algal concentration and (c) temperature on solar/chlorine inactivation of *P. umbonatum*. Conditions: solar irradiance = 900 W/m^2; pH = 6.8 ± 0.2.

9.37 h to 2.74 h, and the k_{max} increased from 0.19 h^{-1} to 1.47 h^{-1}. The increase in algal removal efficiency was mainly due to the higher concentration of oxidants, which produced more active species and promoted algal cell decay with solar irradiance.

Differences in the cell density in the actual water would affect the algal removal efficiency of the oxidant. Fig. 2(b) and S5(b,e) summarized the effect of initial algal density on the removal efficiency of *P. umbonatum* and chlorine decay. The removal efficiency gradually decreased with the increase of initial cell density. Specifically, it was 75 %, 53 % and 28 % at the initial density of 1.0 × 10^4, 2.0 × 10^4 and 3.0 × 10^4 cells/mL, respectively. The SL were 3.65 h, 3.70 h, and 3.62 h, and the k_{max} were 1.11 h^{-1}, 1.28 h^{-1}, and 1.72 h^{-1}, respectively. With the increase in the initial algal density, there was no significant change in the SL, but the k_{max} slightly increased. It can be observed that chlorine decayed more rapidly as algal density increased, indicating that algal cells react with chlorine more rapidly, consistent with an increase in k_{max}. In summary, higher algal density increased the load of solar/chlorine treatment. The oxidant was consumed more quickly at higher algal densities, which accelerated the reaction entry into the trailing phase and reduced the efficiency of algal removal.

Fig. 2(c) summarized the effect of temperature on the effectiveness of solar/chlorine control of *P. umbonatum*. As shown in Fig. S5(f), the rate of chlorine decay gradually increased as the temperature rose. The SL at 20 °C and 25 °C were 4.37 h and 3.65 h, and the k_{max} were 1.07 h^{-1} and 1.11 h^{-1}, respectively. The reaction was slow and the trailing phase appeared later at 20 °C, which was consistent with chlorine decay. The removal efficiency was greatly enhanced when the temperature was raised to 30 °C. The SL decreased to 2.09 h and the k_{max} increased to 3.97 h^{-1}, leading to a removal efficiency of 97 % within 5 h. All physiological activities and biochemical reactions of algae need to be accomplished under certain temperature conditions. In Feitsui Reservoir, the highest density of *P. umbonatum, P. bipes* and *Ceratium furcoides* were found between 24 and 26 °C (Wu and Chou, 1998). Consequently, the increase in algal removal efficiency at 30 °C was attributed to the unfavorable temperature response of the algal cells, further inhibiting algal cell activity.

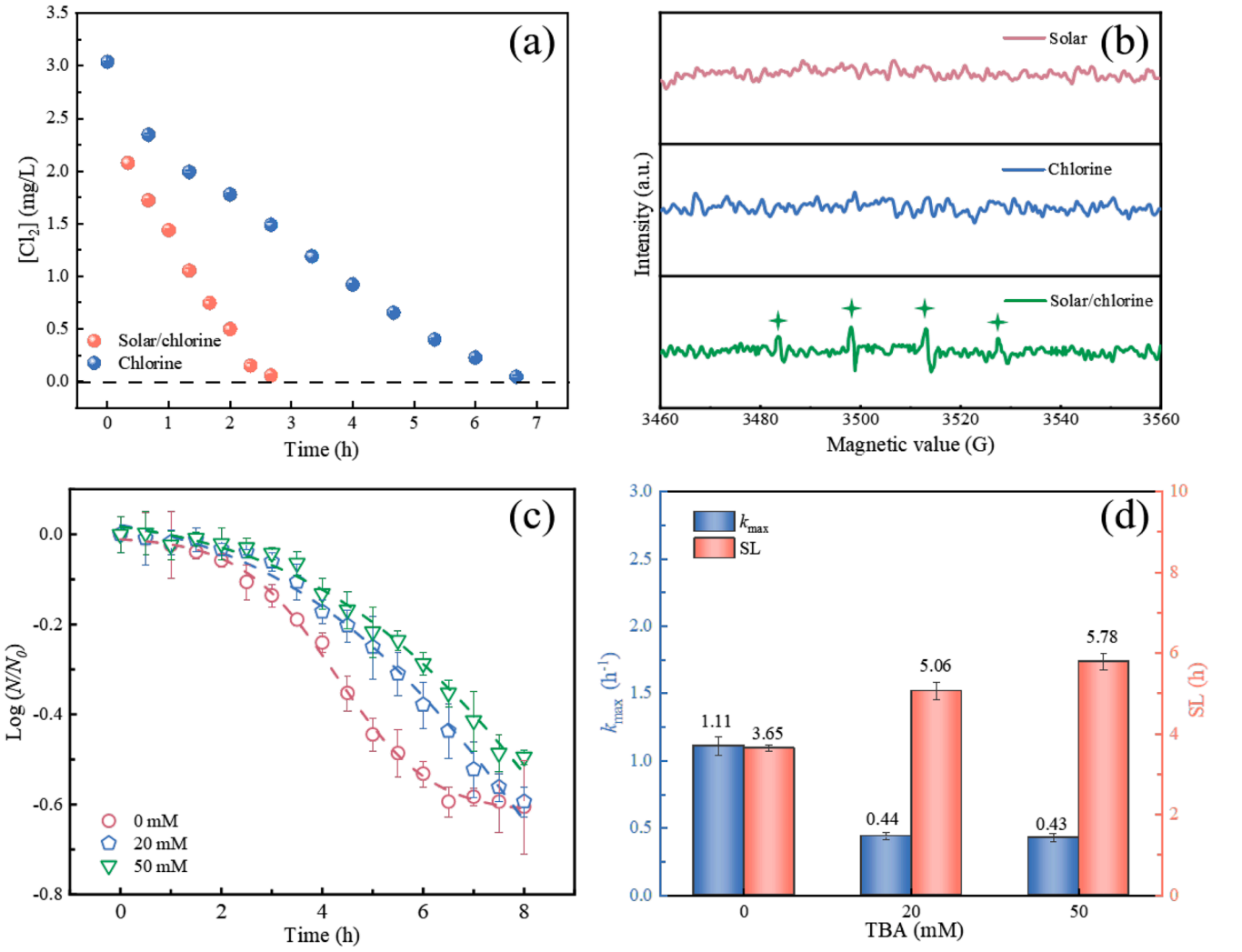

Fig. 3. The roles of reactive species in solar/chlorine treatments: (a) chlorine decay; (b) EPR spectra of chlorine alone, solar alone and solar/chlorine systems; (c) the kinetic fitting curve with TBA; (d) the kinetic fitting parameters with TBA. Conditions: initial *P. umbonatum* concentration = (1.0 ± 0.2)×10^4 cells/mL; $[chlorine]_0$ = 3.0 mg/L; solar irradiance = 900 W/m^2; T = 25±2 °C; pH = 6.8 ± 0.2.

3.3. Inactivation mechanisms analysis

3.3.1. Roles of reactive species

Changes in the concentration of chlorine during treatments with chlorine and solar/chlorine were depicted in Fig. 3(a). There was a decay in the chlorine concentration in the suspension of *P. umbonatum*, with the concentration decaying from 3.0 mg/L to 0 mg/L within 400 min. Nevertheless, the chlorine concentration barely changed with time in 119 media (Fig. S6). Therefore, the decrease in chlorine concentration in algal solution suggested that chlorine interacted with algae. When the solar radiation was added, the time for chlorine to decrease to 0 mg/L was reduced from 400 min to 160 min, indicating that chlorine was photolyzed by solar radiation.

The enhanced effect of solar/chlorine treatment is generally attributed to the generation of reactive species, dominated by O_3 and •OH from chlorine photolysis. (Jia et al., 2023; Yang et al., 2016). However, O_3 was not detected in our reaction system, which is consistent with Wan et al. (2022) and Forsyth et al. (2013). It has also been reported that •OH could accelerate the death of algal cells (Bai et al., 2019b; Chen et al., 2020). In this study, 5,5-dimethyl-1-pyrroline-noxide (DMPO) was utilized as a trapping agent for the Electron Paramagnetic Resonance (EPR) determination and the EPR spectra was shown in Fig. 3(b). No DMPO-•OH signal was detected in the solar alone and chlorine alone systems. However, a characteristic four-peak signal with an intensity ratio of 1:2:2:1 corresponding to the DMPO-•OH adduct was clearly observed in the solar/chlorine system, which indicated that •OH was produced in the solar/chlorine system.

Experiments used different concentrations of tertiary butyl alcohol (TBA) for hydroxyl radical trapping, and the results are shown in Fig. 3 (c, d) and S7 (Tian et al., 2022; Wu et al., 2015). A certain concentration of TBA decreased the efficiency of algae removal. After 20 and 50 mM TBA were added, the SL increased from 3.65 h to 5.06 h and 5.78 h, while the k_{max} decreased from 1.11 h^{-1} to 0.44 h^{-1} and 0.43 h^{-1}, respectively. It was demonstrated that •OH played an important role in the control of algae.

3.3.2. Cell integrity and particle size

The orderly operation of various biochemical activities in algal cells is significantly influenced by cell membranes. The fluorescent microscope images of *P. umbonatum* with various treatment were shown in Fig. S8. Almost all of the cells displayed red fluorescence after 7.5 h of solar radiation alone, indicating that the cell membrane was intact. Green fluorescence appeared after 1.5 h under 3 mg/L chlorine with solar radiation, followed by a sharp decrease in the percentage of intact cells, which were almost completely damaged within 6 h. As shown in Fig. 4(a), the percentage of membrane-damaged cells increased by 45 %

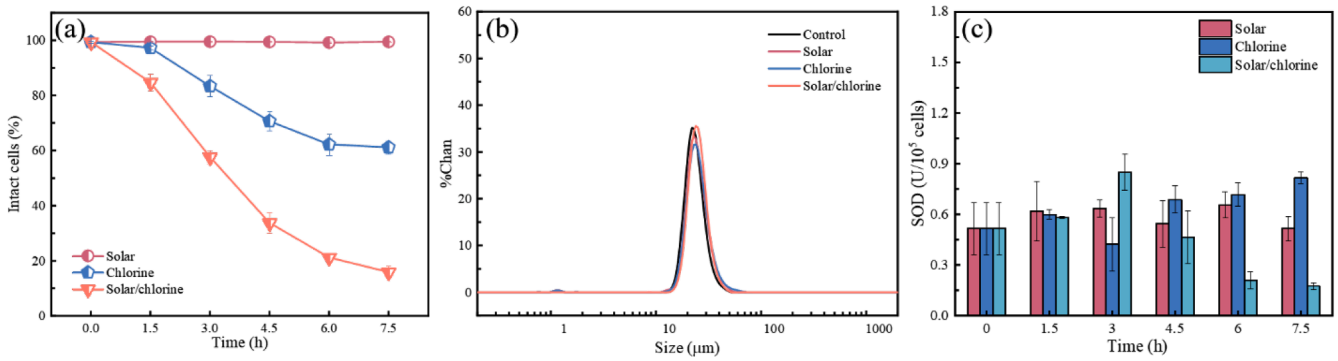

Fig. 4. Variation of (a) membrane permeability, (b) size and (c) SOD of *P. umbonatum* in chlorine alone, solar alone and solar/chlorine treatments. Conditions: initial *P. umbonatum* concentration = (1.0 ± 0.2)×10^4 cells/mL; $[chlorine]_0$ = 3.0 mg/L; solar irradiance = 900 W/m^2; T = 25±2 °C; pH = 6.8 ± 0.2.

compared to chlorine alone. Previous studies have shown that •OH is a non-selective oxidant that can oxidize cell walls or cell membranes, leading to cell rupture (Bai et al., 2019a; Li et al., 2019). The results of cell membrane damage in *P. umbonatum* caused by solar/chlorine were consistent with the algal removal efficiency, suggesting that •OH increased the algal removal efficiency by disrupting the cell membrane.

The change in algal cell particle size after treatment was shown in Fig. 4(b). It can be seen that the peak of the untreated algal cells was located in the range of 20–30 μm, with a volume average of 23.06 μm and a peak size of 22.85 μm, which was consistent with the size of *P. umbonatum* in the previous study (15–43 × 25–40 μm) (Liu et al., 2008), indicating the reliability of the detection method. There was no significant shift in the peak after treatment. The results showed that although the cell membrane of *P. umbonatum* was damaged, the algal cells did not completely disintegrate and maintained their original shapes (Wang et al., 2024).

3.3.3. Antioxidant enzyme activity

In this study, SOD enzyme activity was measured using a microplate reader combined with a SOD kit. The change in SOD enzyme activity with time during algal removal by different methods was depicted in Fig. 4(c). SOD enzyme activity only slightly increased when exposed to solar radiation alone, suggesting that the algae cells were not suffering severe stress. SOD enzyme activity increased from 0.517 U/10^5cells to 0.817 U/10^5cells after treatment with 3 mg/L chlorine alone for 7.5 h, indicating that the SOD enzyme activity was increased to inhibit the production of free radicals (Zhang et al., 2022). In solar/chlorine treatment, SOD enzyme activity increased to 0.847 U/10^5cells after 3 h and then gradually decreased to 0.176 U/10^5cells. The elevation of SOD enzyme activity in the initial phase of the study indicated that the intracellular reactive oxygen species (ROS) level was elevated, while the significant decrease observed later could be attributed to the inability to scavenge excess free radicals in a timely manner, leading to severe damage or even death (Ebenezer and Ki, 2013). Consistent with the changes in cell membrane integrity, the degree of oxidative damage caused by the three treatments to *P. umbonatum* was as follows: solar/-chlorine > chlorine > solar, suggesting that •OH produced by the solar/chlorine system induced higher oxidative stress.

3.3.4. Algal cell morphology

In order to observe the morphology of *P. umbonatum* before and after treatment, images of *P. umbonatum* after 8 h of treatment with three different methods were taken using SEM with magnifications of 3000, 1000 and 500 times, respectively, as shown in Fig. 5. The untreated cells

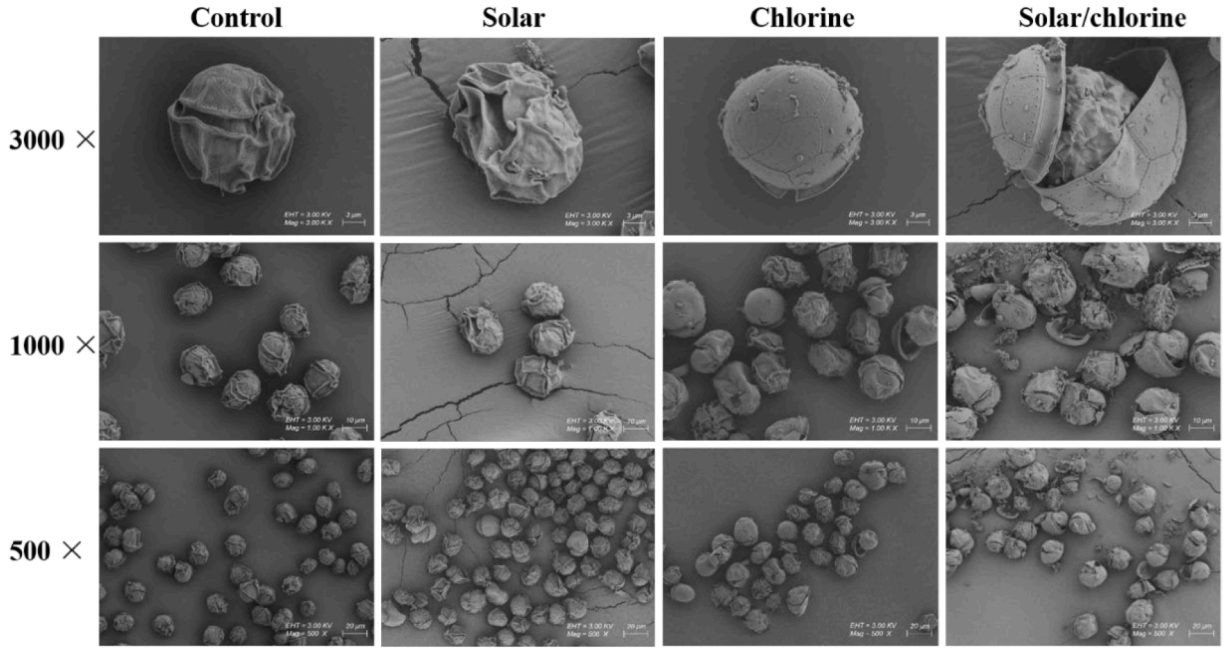

Fig. 5. SEM photos of *P. umbonatum* before and after 8 h treatments. Conditions: initial *P. umbonatum* concentration = (1.0 ± 0.2)×10^4 cells/mL; $[chlorine]_0$ = 3.0 mg/L; solar irradiance = 900 W/m^2; T = 25±2 °C; pH = 6.8 ± 0.2.

of *P. umbonatum* showed an oval shape with an obvious platy structure and reticulate pattern on the plates. Some of the algal cells appeared wrinkled due to the dehydration caused by different concentrations of ethanol during the sampling process, but they remained mostly intact and full, with no impurity particles outside the cells. After treatment with 3 mg/L chlorine alone, the surface of partial algal cells appeared swelled or ruptured, indicating that the membrane of the algal cells was damaged. The surface of algal cells was seriously deformed, and almost all the attacked cells were cracked in the solar/chlorine system. Obvious particle-like or piece-like material attached to the surface of the algal cells was observed, which was speculated to be the release of intracellular material after algal cells decay (Ahn et al., 2013). According to the SEM images magnified 3000 times, it can be observed that although the algal cell structure was altered, the cells were not completely cleaved into fragments and even aggregated due to the presence of released polymers, which was consistent with the particle size results in Section 3.3.2.

3.3.5. Photosynthetic activity

Photosynthesis is one of the most important reactions in the growth of algal cells. As shown in Fig. 6, solar/chlorine exhibited an obvious inhibitory effect on the photosynthetic activity of *P. umbonatum*. The chl-a concentration of algal cells remained at the initial level (155.47 μg/L) without significant reduction after solar radiation alone. Following treatment with 3 mg/L chlorine for 7.5 h, the concentration of chl-a decreased to 88.90 μg/L. In contrast, 30.44 μg/L of chl-a was obtained after solar/chlorine treatment, indicating that chlorine affected the concentration of photosynthetic pigments, with solar radiation further accelerating the process.

As depicted in Fig. 6 (b, c), there was a slight reduction in Fv/Fm and Y(II) after treatment by solar alone and 3 mg/L chlorine alone, with Fv/Fm and Y(II) decreasing to 0.398 and 0.312 after 5 h of solar alone, respectively. The Fv/Fm and Y(II) decreased to 0.332 and 0.262 after 5 h of chlorine alone, respectively. It was in line with the changes in chl-a concentration, highlighting the greater impact of chlorine on photosynthetic activity compared to solar radiation alone. Both Fv/Fm and Y(II) decreased to 0 within 3 h after solar/chlorine treatment, which had a more severe effect on photosynthetic activity compared to solar and chlorine alone. Similarly, the ETR of the algal cells followed the same pattern, with the ETR decreasing in the following order: solar/chlorine>chlorine>solar. The ETR decreased from 11.3 to 6.8 and 2.5 after solar radiation and chlorine treatment alone for 5 h, and to 0 within 3 h in the case of solar/chlorine. It has been demonstrated that •OH can penetrate the cell membrane, causing damage to algal cells (Bai et al.,

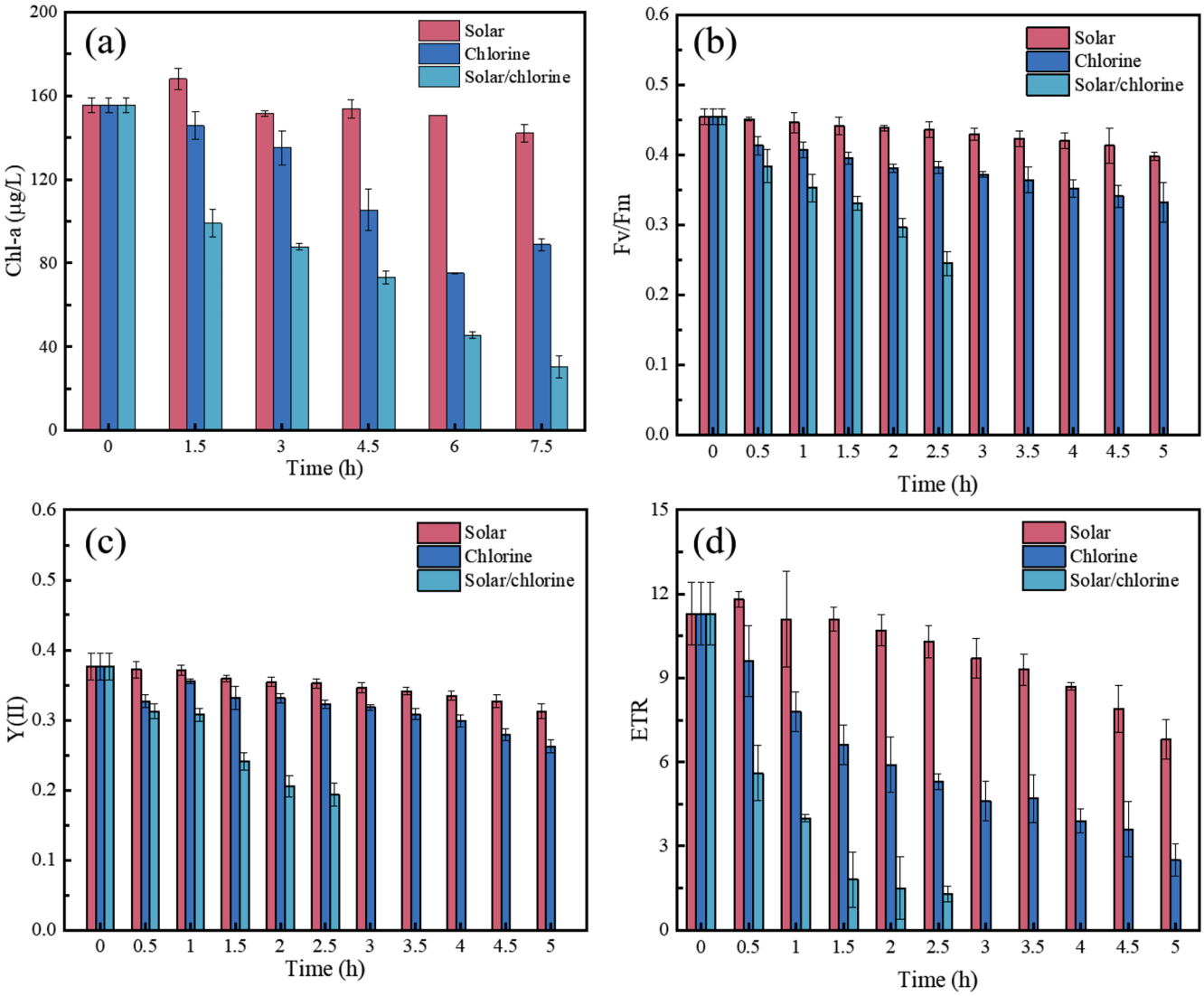

Fig. 6. Variation of (a) Chl-a, (b) Fv/Fm, (c)Y(II) and (d) ETR of *P. umbonatum* in chlorine alone, solar alone and solar/chlorine treatments. Conditions: initial *P. umbonatum* concentration = (1.0 ± 0.2)×10^4 cells/mL; $[chlorine]_0$ = 3.0 mg/L; solar irradiance = 900 W/m^2; T = 25±2 °C; pH = 6.8 ± 0.2.

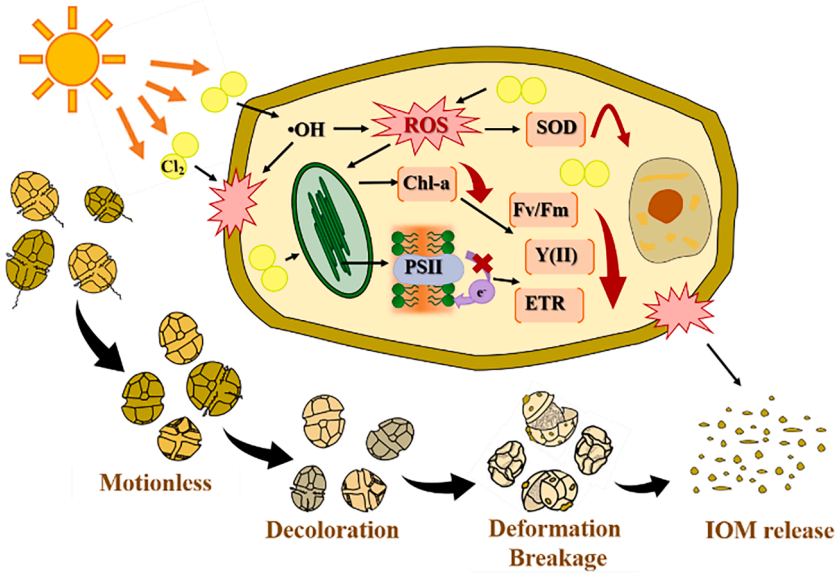

Fig. 7. Diagram of the algal apoptosis during solar/chlorine treatment.

2019a). •OH generated by solar/chlorine treatment accelerated the reduction of photosynthetic pigments and electron transfer rates in algal cells, thus disrupting photosynthetic capacity and accelerating cellular death.

3.3.6. Discussion on the algal apoptosis

The mechanism of solar/chlorine control of *P. umbonatum* was summarized in Fig. 7, where the gradual motionlessness, decoloration, and rupture of algal cells were observed under a microscope. The death of *P. umbonatum* primarily occurred in the following ways: (1) algae cells lost the ability to move rapidly and remain stationary; (2) the morphology of the algal cells was damaged and the cell membranes were severely disrupted; (3) intracellular oxidation in the algal cells was increased, which manifested as a first increase and then a gradual decrease in the activity of antioxidant enzymes; (4) photosynthesis in algal cells was inhibited. The enhanced removal efficiency of *P. umbonatum* was attributed to the co-oxidation of chlorine and •OH. The attack of chlorine and •OH on the cell membrane led to a decrease in membrane integrity, an elevation in intracellular ROS, and heightened morphological damage to algal cells, which in turn enhanced the removal effect of solar/chlorine on *P. umbonatum*.

3.4. Regrowth of algae after inactivation

To monitor algal cell regrowth, algal solutions containing culture medium after different treatments were transferred to an incubator. Fig. 8(a) depicted the regrowth of *P. umbonatum* after 8 h of treatment under three different conditions. Following solar treatment alone, algal cells grew normally and cell density increased by 0.45×10^4 cells/mL approximately within 7 d The density gradually decreased to 0.55×10^4 cells/mL during the first 4 h and then remained stable with chlorine alone treatment, whereas cell densities were essentially unchanged after solar/chlorine treatment, and no regrowth was observed. As depicted in Fig. 8(b), the DOC concentration in the reaction system gradually

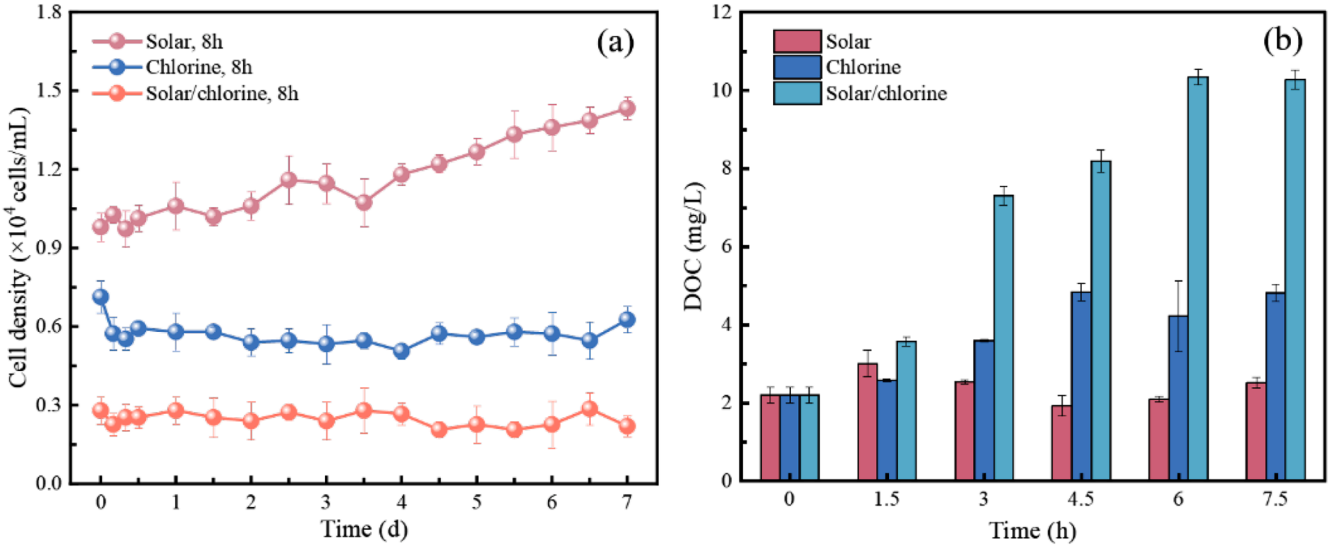

Fig. 8. (a)Representative regrowth curves of *P. umbonatum* after different treatment and (b) changes in DOC of the system in chlorine alone, solar alone and solar/chlorine treatments. Conditions: initial *P. umbonatum* concentration = $(1.0 \pm 0.2) \times 10^4$ cells/mL; $[\text{chlorine}]_0 = 3.0$ mg/L; solar irradiance = 900 W/m^2; $T = 25 \pm 2$ °C; pH = 6.8 ± 0.2.

increased from 2.19 mg/L to 4.82 mg/L and 10.28 mg/L after treatment by chlorine and solar/chlorine, respectively. It has been shown that organic matter can react with chlorine to form disinfection by-products. However, no DOC reduction was observed due to the rapid decay of chlorine in the system (Yeom et al., 2021). UVA-like humic and tryptophan-like components were predominantly detected in the chlorine and solar/chlorine systems (Fig. S9 and S10), whereas tryptophan-like component increased more dramatically and was the main component of the intracellular organic matter of *P. umbonatum* (Fig. S11). This indicated that the increase of DOC in the system primarily stems from the release of intracellular organic matter, further confirming the thoroughness of algal removal by solar/chlorine treatment and explaining the absence of algal regrowth. On the other hand, dinoflagellate cells form cysts in unfavorable environments and are unable to regenerate for a brief period of time (Matsuoka and Fukuyo, 2000).

3.5. Applications in natural conditions

3.5.1. Effectiveness in real water matrices

In order to further investigate the removal efficiency of solar/chlorine on *P. umbonatum* in a real water environment, water from Sanhekou Reservoir was selected as the actual water (Table S2). The results were shown in Fig. 9(a). The k_{max} in the solar/chlorine system was 0.33 h^{-1} in the water from Sanhekou reservoir, which was 70 % lower than that in the 119 medium (1.11 h^{-1}), and the SL was prolonged to 6.86 h compared to that in the 119 medium (3.65 h). The removal efficiency was 75 % and 56 % after 8 h of treatment with solar/chlorine in 119 medium and real water, respectively. The background material in real water is more complex than in the 119 medium, with higher concentrations of dissolved organic matter (DOM), metal ions, etc., which consume oxidants and reduce algal removal efficiency (Wang et al., 2017b). Moreover, the background substance and its complexes acted as shading agents in real water (Kohantorabi et al., 2019).

3.5.2. Inactivation in natural solar radiation

Simulated solar had a certain strengthening effect on the removal efficiency of algae by chlorine treatment. In order to verify whether natural solar radiation has the same effect, experiments were conducted in September and October under natural solar radiation. Natural solar intensity was measured with a solar power meter. The temperature of the system was kept in the range of 25–30 °C using a water bath.

Fig. 9(b) demonstrated the effect of natural solar/chlorine on the control of *P. umbonatum* in September, and the removal rate of algal cells reached 97 % after 4 h of solar alone treatment because of the high UV index (solar irradiance = 780–930 W/m^2, UV index = 7). This is consistent with the characteristic of *P. umbonatum* that it prefers thin light but not intense sunlight, and excessive solar intensity would destroy the photosynthetic capacity and induce cell death (Heaney and Furnass, 1980; Heaney and Talling, 1980; Regel, 2004). The addition of chlorine resulted in 99 % of algal cell removal at 4 h, which was slightly higher than solar radiation alone. There were no significant differences in k_{max} and SL between solar/chlorine and solar alone conditions.

It is difficult to maintain the normal growth state for *P. umbonatum* and gather to form a water bloom under high solar intensity. The experiment was carried out under lower intensity in October (solar irradiance = 650–860 W/m^2, UV index = 1), and the results were shown in Fig. 9(c). The removal efficiency was 20 % after 6 h of chlorine treatment alone, which was not significantly different from the results of the experiment in September. After 6 h of solar radiation alone, the removal efficiency of algae was 33 %, which was much lower than that of high solar intensity. The algae can move to 3–4 m below the surface of the water in the reservoir to avoid direct solar radiation and grow normally under this intensity. The removal efficiency reached 87 % after 6 h in natural solar/chlorine system. The k_{max} in the solar/chlorine system (0.58 h^{-1}) was much higher than solar (0.18 h^{-1}) and chlorine alone (0.42 h^{-1}), while the SL (2.32 h) was much lower than solar (6.49 h) and chlorine alone (8.28 h). Due to the higher UV intensity of natural solar, both solar alone and solar/chlorine show better algae removal than simulated solar. It has been demonstrated that the algae removal efficiency can be enhanced by natural solar/chlorine as well. Consequently, employing chlorine oxidants on sunny days for emergency control is more successful.

4. Conclusions

The main conclusions can be summarized as follows:

(1) The removal efficiency of solar alone on *P. umbonatum* was insignificant, while the solar/chlorine treatment exhibited superior removal efficiency compared to solar or chlorine treatment alone with the SL reduction factor and k_{max} enhancement factor of 2.80 and 3.8.
(2) The removal efficiency of algae by solar/chlorine gradually increased with the chlorine dosage, but it decreased with algal density. Moreover, an increase in temperature to 30 °C significantly enhanced removal efficiency due to the unfavorable conditions for *P. umbonatum* survival.
(3) Attacks on cell membranes by chlorine and •OH resulted in a decrease in cell membrane integrity, leading to an increase in intracellular ROS and an inhibition of photosynthetic and antioxidant systems, which in consequence enhanced the removal effect of solar/chlorine on *P. umbonatum*.
(4) The release of IOM was detected in the solar/chlorine system, indicating that the algal cells were severely damaged and no regeneration was observed.
(5) The algal removal efficiency of solar/chlorine in real water was reduced compared to 119 medium, which was mainly due to background material in the real water substrate that consuming the oxidant or acting as a shading agent. Moreover, natural solar

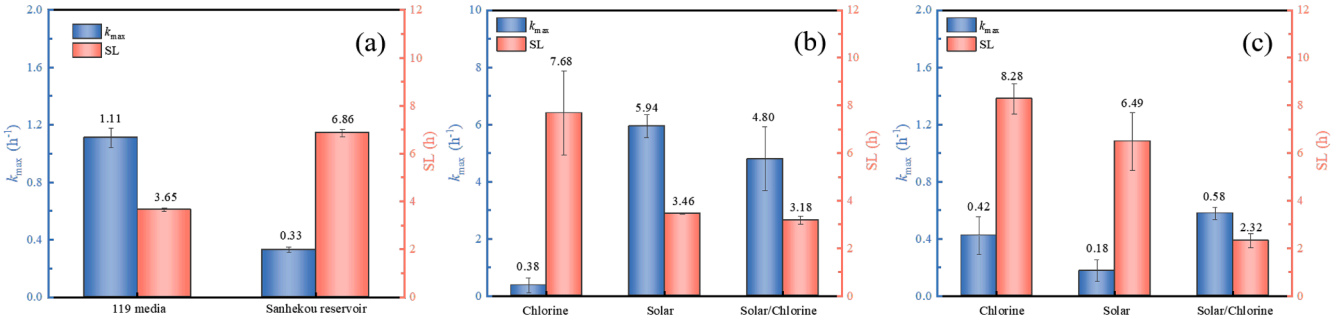

Fig. 9. Inactivation kinetic parameters of *P. umbonatum* in (a) real water matrices and (b)(c) natural solar radiation: (b) September; (c) October. Conditions: initial *P. umbonatum* concentration = (1.0 ± 0.2) × 10^4 cells/mL; $[chlorine]_0$ = 3.0 mg/L; T = 25±2 °C.

radiation was demonstrated to have the same enhancing effect as simulated solar, with a removal efficiency of 87 % after 6 h.

CRediT authorship contribution statement

Ru Wang: Writing – original draft, Methodology, Investigation, Data curation. **Ya Cheng:** Validation, Supervision, Conceptualization. **Qiqi Wan:** Writing – review & editing, Supervision, Methodology, Funding acquisition. **Ruihua Cao:** Supervision, Data curation. **Jie Cai:** Methodology, Investigation. **Tinglin Huang:** Supervision, Funding acquisition. **Gang Wen:** Writing – review & editing, Validation, Supervision, Funding acquisition, Conceptualization.

Declaration of competing interest

The authors declare that they have no known competing financial interests or personal relationships that could have appeared to influence the work reported in this paper.

Data availability

Data will be made available on request.

Acknowledgements

This research was funded by the Natural Science Foundation of China (Grant No. 52370018, 52300010), Shaanxi Provincial Key Scientific and Technological Innovation Team (2023-CX-TD-32), China Postdoctoral Science Foundation (No. 2023MD734208), Research Program of Youth Innovation Team (Shaanxi Provincial Department of Education, No. 23JP077), and Technology Innovation Leading Program of Shaanxi (No.2023GXLH-058).

Supplementary materials

Supplementary material associated with this article can be found, in the online version, at doi:10.1016/j.watres.2024.122275.

References

Ahn, S., Peterson, T.D., Righter, J., Miles, D.M., Tratnyek, P.G., 2013. Disinfection of ballast water with iron activated persulfate. Environ. Sci. Technol. 47 (20), 11717–11725.

Bai, M., Yu, Y., Cheng, J., Ji, Z., Li, J., 2019a. OH degraded 2-Methylisoborneol during the removal of algae-laden water in a drinking water treatment system: comparison with ClO_2. Chemosphere 236, 124342.

Bai, M., Zheng, Q., Zheng, W., Li, H., Lin, S., Huang, L., Zhang, Z., 2019b. •OH inactivation of Cyanobacterial blooms and degradation of toxins in drinking water treatment system. Water Res. 154, 144–152.

Burson, A., Matthijs, H.C., de Bruijne, W., Talens, R., Hoogenboom, R., Gerssen, A., Visser, P.M., Stomp, M., Steur, K., van Scheppingen, Y., 2014. Termination of a toxic Alexandrium bloom with hydrogen peroxide. Harmful Algae 31, 125–135.

Cao, L., Wang, J., Wang, Z., Yu, S., Cheng, Y., Ma, J., Xie, P., 2022. Inactivation of *Microcystis Aeruginosa* by peracetic acid combined with ultraviolet: performance and characteristics. Water Res. 208, 117847.

Carty, S., Parrow, M.W., 2015. Dinoflagellates. In: Wehr, J.D., Sheath, R.G., Kociolek, J. P. (Eds.), Freshwater Algae of North America (Second Edition), Aquatic Ecology. Academic Press, Boston, pp. 773–807.

Chen, Y., Bai, F., Li, Z., Xie, P., Wang, Z., Feng, X., Liu, Z., Huang, L.-Z., 2020. UV-assisted chlorination of algae-laden water: cell lysis and disinfection byproducts formation. Chem. Eng. J. 383, 123165.

Chen, Z., Li, J., Chen, M., Koh, K.Y., Du, Z., Gin, K.Y.-H., He, Y., Ong, C.N., Chen, J.P., 2021. *Microcystis aeruginosa* removal by peroxides of hydrogen peroxide, peroxymonosulfate and peroxydisulfate without additional activators. Water Res. 201, 117263.

Daly, R.I., Ho, L., Brookes, J.D., 2007. Effect of chlorination on *Microcystis aeruginosa* cell integrity and subsequent microcystin release and degradation. Environ. Sci. Technol. 41 (12), 4447–4453.

Ebenezer, V., Ki, J.-S., 2013. Physiological and biochemical responses of the marine dinoflagellate *Prorocentrum minimum* exposed to the oxidizing biocide chlorine. Ecotoxicol. Environ. Saf. 92, 129–134.

Forsyth, J.E., Zhou, P.R., Mao, Q.X., Asato, S.S., Meschke, J.S., Dodd, M.C., 2013. Enhanced inactivation of *Bacillus subtilis* spores during solar photolysis of free available chlorine. Environ. Sci. Technol. 47 (22), 12976–12984.

Geeraerd, A.H., Valdramidis, V.P., Van Impe, J.F., 2005. GInaFiT, a freeware tool to assess non-log-linear microbial survivor curves. Int. J. Food Microbiol. 102 (1), 95–105.

Ginzburg, B., Chalifa, I., Zohary, T., Hadas, O., Dor, I., Lev, O., 1998. Identification of oligosulfide odorous compounds and their source in the Lake of Galilee. Water Res. 32 (6), 1789–1800.

Gong, D., 2022. Study On the Control Technologies of Chlorination Typical Algal-Derived Disinfection By-Products of Water Treatment Plant in Chongqing. MasterChongqing University.

Han, J., Cao, R., Li, K., Wang, S., Ji, G., Xu, H., Wang, J., Huang, T., Wen, G., 2022. Change of algal organic matter under different dissolved oxygen and pressure conditions and its related disinfection by-products formation potential in metalimnetic oxygen minimum. Water Res. 226, 119216.

Heaney, S., Furnass, T., 1980. Laboratory models of diel vertical migration in the dinoflagellate *Ceratium hirundinella*. Freshw. Biol. 10 (2), 163–170.

Heaney, S., Talling, J., 1980. Dynamic aspects of dinoflagellate distribution patterns in a small productive lake. J. Ecol. 68 (1), 75–94.

Holm-Hansen, O., Riemann, B., 1978. Chlorophyll a determination: improvements in methodology. Oikos 30, 438–447.

Hu, X., Su, H., Xu, Y., Xu, W., Li, S., Huang, X., Cao, Y., Wen, G., 2020. Algicidal properties of fermentation products from *Bacillus cereus* strain JZBC1 dissolving dominant dinoflagellate species *Scrippsiella trochoidea, Prorocentrum micans*, and *Peridinium umbonatum*. Biologia 75 (11), 2015–2024.

Huang, T., Wen, C., Wang, S., Wen, G., Li, K., Zhang, H., Wang, Z., 2022. Controlling spring dinoflagellate blooms in a stratified drinking water reservoir via artificial mixing: effects, mechanisms, and operational thresholds. Sci. Total Environ. 847, 157400.

Ichikawa, S., Wakao, Y., Fukuyo, Y., 1992. Extermination efficacy of hydrogen peroxide against cysts of red tide and toxic dinoflagellates, and its adaptability to ballast water of cargo ships. Nippon Suisan Gakkaishi 58 (12), 2229–2233.

Iseri, Y., Kawabata, Z.i., Sasaki, M., 1994. Development of a boat equipped with UV lamps for suppression of freshwater red tide in a reservoir. Jpn. J. Water Treat. Biol. 29 (2), 61–70.

Jia, H., Ma, X.Y., Lin, Y., Yang, S., An, Y., Chen, Y., Wang, X.C., 2023. Evolvement of carbamazepine under solar irradiation in the presence of chlorine: efficiency, influences, degradation pathways and ecotoxicity. Chem. Eng. J. 461, 142106.

Jutaporn, P., Armstrong, M.D., Coronell, O., 2020. Assessment of C-DBP and N-DBP formation potential and its reduction by MIEX DOC and MIEX GOLD resins using fluorescence spectroscopy and parallel factor analysis. Water Res. 172, 115460.

Kang, Y.K., Cho, S.Y., Kang, Y.H., Katano, T., Jin, E.S., Kong, D.S., Han, M.S., 2008. Isolation, identification and characterization of algicidal bacteria against *Stephanodiscus hantzschii* and *Peridinium bipes* for the control of freshwater winter algal blooms. J. Appl. Phycol. 20 (4), 375–386.

Kawabata, Z.i., Sasaki, K., Iseri, Y., Ochiai, M., 1990. Effet of ultraviolet radiation on the survival of the dinoflagellate *Peridinium bipes* causing freshwater red tide in reservoirs. Jpn. J. Water Treat. Biol. 26 (2), 17–22.

Kohantorabi, M., Giannakis, S., Gholami, M.R., Feng, L., Pulgarin, C., 2019. A systematic investigation on the bactericidal transient species generated by photo-sensitization of natural organic matter (NOM) during solar and photo Fenton disinfection of surface waters. Appl. Catal. B-Environ. 244, 983–995.

Li, H., Bai, M., Yang, X., Zhong, Z., Gao, M., Tian, Y., 2019. OH pre-treatment of algae blooms and degradation of microcystin-LR in a drinking water system of 480 m^3/day: comparison with ClO_2. Chem. Eng. J. 367, 189–197.

Li, L., Yu, T., Cheng, S., Li, J., Li, C., Wang, G., Tan, D., Li, L., Zhang, H., Zhang, X., 2022. Removal of cyanobacteria using novel pre-pressurized coagulation: the effect of cellular properties and algogenic organic matter characteristics. Sep. Purif. Technol. 282, 119927.

Li, S., Dao, G.H., Tao, Y., Zhou, J., Jiang, H.S., Xue, Y.M., Yu, W.W., Yong, X.L., Hu, H.Y., 2020. The growth suppression effects of UV-C irradiation on *Microcystis aeruginosa* and *Chlorella vulgaris* under solo-culture and co-culture conditions in reclaimed water. Sci. Total Environ. 713, 136374.

Liu, G., Hu, S., Chu, G., Hu, Z., 2008. Study on freshwater genus *Peridinium* (Dinophyta) from China. Acta Phytotaxonomica Sinica 46 (5), 754–771.

Matsuoka, K., Fukuyo, Y., 2000. Technical Guide For Modern Dinoflagellate Cyst Study. WESTPAC-HAB Asian Natural Environmental Science Center, Tokyo.

Oshima, Y., Minami, H., Takano, Y., Yasumoto, T., 1987. Ichthyotoxins in a freshwater dinoflagellate *Peridinium polonicum*. In: Okaichi, T., Anderson, D.M., Nemoto, T. (Eds.), Red tides: Biology, Environmental science, and Toxicology. Elsevier Science Publishing, pp. 375–378.

Pápista, É., Ács, É., Böddi, B., 2002. Chlorophyll-a determination with ethanol - a critical test. Hydrobiologia 485 (1–3), 191–198.

Piel, T., Sandrini, G., White, E., Xu, T., Schuurmans, J.M., Huisman, J., Visser, P.M., 2019. Suppressing cyanobacteria with hydrogen peroxide is more effective at high light intensities. Toxins (Basel) 12 (1), 18.

Regel, R.H., 2004. Vertical migration, entrainment and photosynthesis of the freshwater dinoflagellate *Peridinium cinctum* in a shallow urban lake. J. Plankton Res. 26 (2), 143–157.

Rodríguez-Chueca, J., Giannakis, S., Marjanovic, M., Kohantorabi, M., Gholami, M.R., Grandjean, D., de Alencastro, L.F., Pulgarín, C., 2019. Solar-assisted bacterial disinfection and removal of contaminants of emerging concern by Fe^{2+}-activated HSO_5^- vs. $S_2O_8^{2-}$ in drinking water. Appl. Catal. B 248, 62–72.

Roset, J., Gibello, A., Aguayo, S., Domínguez, L., Álvarez, M., Fernández-Garayzabal, J., Zapata, A., Muñoz, M., 2002. Mortality of rainbow trout [Oncorynchus mykiss

(Walbaum)] associated with freshwater dinoflagellate bloom [*Peridinium polonicum* (Woloszynska)] in a fish farm. Aquac. Res. 33 (2), 141–145.
Song, Y., Shen, L., Zhang, L., Li, J., Chen, M., 2021. Study of a hydrodynamic threshold system for controlling dinoflagellate blooms in reservoirs. Environ. Pollut. 278, 116822.
Tian, S., Wang, G., Liu, Y., Qi, J., Tian, L., Ma, J., Wang, L., Wen, G., 2022. Highly effective dehalogenation and detoxification of trihalophenols by activated peroxydisulfate with black carbon derived from coal tar. Chem. Eng. J. 440, 135958.
Tian, X., Li, Y., Xu, H., Pang, Y., Zhang, J., Pei, H., 2021. Fe^{2+} activating sodium percarbonate (SPC) to enhance removal of Microcystis aeruginosa and microcystins with pre-oxidation and in situ coagulation. J. Hazard. Mater. 412, 125206.
Wan, Q., Wen, G., Cao, R., Zhao, H., Xu, X., Xia, Y., Wu, G., Lin, W., Wang, J., Huang, T., 2020. Simultaneously enhance the inactivation and inhibit the photoreactivation of fungal spores by the combination of UV-LEDs and chlorine: kinetics and mechanisms. Water Res. 184, 116143.
Wan, Q., Xia, Y., Li, Y., Wu, G., Wang, J., Huang, T., Wen, G., 2022. Enhanced solar inactivation of fungal spores by addition of low-dose chlorine: efficiency and mechanism. Water Res. 222, 118964.
Wang, D.H., Li, L., Zhu, C.W., Wang, Z.Y., Xie, P., 2017a. Combined application of natural sunlight and hydrogen peroxide on the removal of harmful cyanobacteria. IOP Conf. Ser. 81 (1), 012068.
Wang, L., Ye, C., Guo, L., Chen, C., Kong, X., Chen, Y., Shu, L., Wang, P., Yu, X., Fang, J., 2021. Assessment of the uv/chlorine process in the disinfection of *Pseudomonas aeruginosa*: efficiency and mechanism. Environ. Sci. Technol. 55 (13), 9221–9230.
Wang, R., Wang, S., Cao, R., Han, J., Huang, T., Wen, G., 2024. The apoptosis of *Chlorella vulgaris* and the release of intracellular organic matter under metalimnetic oxygen minimum conditions. Sci. Total Environ. 907, 168001.
Wang, W.L., Wu, Q.Y., Li, Z.M., Lu, Y., Du, Y., Wang, T., Huang, N., Hu, H.Y., 2017b. Light-emitting diodes as an emerging UV source for UV/chlorine oxidation: carbamazepine degradation and toxicity changes. Chem. Eng. J. 310, 148–156.
Wen, G., Liang, Z., Xu, X., Cao, R., Wan, Q., Ji, G., Lin, W., Wang, J., Yang, J., Huang, T., 2020. Inactivation of fungal spores in water using ozone: kinetics, influencing factors and mechanisms. Water Res. 185, 116218.
Wu, J., Chou, J., 1998. Dinoflagellate associations in Feitsui Reservoir, Taiwan. Botanical Bull. Academia Sinica. 39 (2), 137–145.
Wu, X., Gu, X., Lu, S., Qiu, Z., Sui, Q., Zang, X., Miao, Z., Xu, M., 2015. Strong enhancement of trichloroethylene degradation in ferrous ion activated persulfate system by promoting ferric and ferrous ion cycles with hydroxylamine. Sep. Purif. Technol. 147, 186–193.
Xia, Y., Wan, Q., Xu, X., Cao, R., Li, Y., Wang, J., Xu, H., Huang, T., Wen, G., 2022. Solar disinfection of fungal spores in water: kinetics, influencing factors, mechanisms and regrowth. Chem. Eng. J. 428, 132065.
Xie, P.C., Ma, J., Fang, J.Y., Guan, Y.H., Yue, S.Y., Li, X.C., Chen, L.W., 2013. Comparison of permanganate preoxidation and preozonation on algae containing water: cell integrity, characteristics, and chlorinated disinfection byproduct formation. Environ. Sci. Technol. 47 (24), 14051–14061.
Xu, H., Pang, Y., Li, Y., Zhang, S., Pei, H., 2021. Using sodium percarbonate to suppress vertically distributed filamentous cyanobacteria while maintaining the stability of microeukaryotic communities in drinking water reservoirs. Water Res. 197, 117111.
Xu, J., Wu, X., Yang, Y., Xu, S., Kang, Y., Fu, X., Yue, H., Shi, J., Wu, Z., 2016. Changes in growth, photosynthesis and chlorophyll fluorescence in the freshwater dinoflagellate *Peridinium umbonatum* (Peridiniales, Pyrrophyta) in response to different temperatures. Phycologia 55 (4), 469–477.
Yang, B., Kookana, R.S., Williams, M., Du, J., Doan, H., Kumar, A., 2016. Removal of carbamazepine in aqueous solutions through solar photolysis of free available chlorine. Water Res. 100, 413–420.
Ye, C., Chen, C., Zhang, K., Wu, X., Cai, W.-F., Feng, M., Yu, X., 2023. Solar/periodate-triggered rapid inactivation of *Microcystis aeruginosa* by interrupting the Calvin-Benson cycle. Environ. Int. 180, 108204.
Yeom, Y., Han, J., Zhang, X., Shang, C., Zhang, T., Li, X., Duan, X., Dionysiou, D.D., 2021. A review on the degradation efficiency, DBP formation, and toxicity variation in the UV/chlorine treatment of micropollutants. Chem. Eng. J. 424, 130053.
Yu, B., Zhang, Y., Wu, H., Yan, W., Meng, Y., Hu, C., Liu, Z., Ding, J., Zhang, H., 2024. Advanced oxidation processes for synchronizing harmful microcystis blooms control with algal metabolites removal: from the laboratory to practical applications. Sci. Total Environ. 906, 167650.
Zhang, H., Zong, R., He, H., Huang, T., 2022. Effects of hydrogen peroxide on *Scenedesmus obliquus*: cell growth, antioxidant enzyme activity and intracellular protein fingerprinting. Chemosphere 287, 132185.
Zhou, P., Di Giovanni, G.D., Meschke, J.S., Dodd, M.C., 2014. Enhanced inactivation of *Cryptosporidium parvum* oocysts during solar photolysis of free available chlorine. Environ. Sci. Technol. Lett. 1 (11), 453–458.
Zhou, T., Cao, H., Zheng, J., Teng, F., Wang, X., Lou, K., Zhang, X., Tao, Y., 2020. Suppression of water-bloom cyanobacterium *Microcystis aeruginosa* by algaecide hydrogen peroxide maximized through programmed cell death. J. Hazard. Mater. 393, 122394.
Zhou, T., Zheng, J., Cao, H., Wang, X., Lou, K., Zhang, X., Tao, Y., 2018. Growth suppression and apoptosis-like cell death in *Microcystis aeruginosa* by H_2O_2: a new insight into extracellular and intracellular damage pathways. Chemosphere 211, 1098–1108.